

# UC Irvine

## UC Irvine Previously Published Works

### Title

Modeling Aberrant Wound Healing Using Tissue-Engineered Skin Constructs and Multiphoton Microscopy

### Permalink

<https://escholarship.org/uc/item/5zj2t857>

### Journal

Facial Plastic Surgery & Aesthetic Medicine, 6(3)

### ISSN

2689-3614

### Authors

Torkian, Behrooz A  
Yeh, Alvin T  
Engel, Rodney  
[et al.](#)

### Publication Date

2004-05-01

### DOI

10.1001/archfaci.6.3.180

### Copyright Information

This work is made available under the terms of a Creative Commons Attribution License, available at <https://creativecommons.org/licenses/by/4.0/>

Peer reviewed

# Modeling Aberrant Wound Healing Using Tissue-Engineered Skin Constructs and Multiphoton Microscopy

Behrooz A. Torkian, MD; Alvin T. Yeh, PhD; Rodney Engel, BA; Chung-Ho Sun, PhD; Bruce J. Tromberg, PhD; Brian J. F. Wong, MD, PhD

**Background:** Keloids and hypertrophic scars result from aberrant wound healing and remain a potential complication of any surgical procedure or trauma. Investigation of aberrant wound healing has been limited to the study of growth factors, collagen precursors, and DNA synthesis in simple in vitro systems, which necessitate removal or destruction of cells or factors in the growth environment of cell cultures. Multiphoton microscopy (MPM) can use endogenous chromophores such as collagen and nicotinamide adenine dinucleotide hydrogenase to produce thin optical sections of thick living tissues without the use of dyes or stains. Endogenous second-harmonic-generation (SHG) signals in collagen can be collected to form an MPM image.

**Objective:** To present a novel wound-healing model used to investigate keloid-derived fibroblast activity and collagen production in the same intact tissue-engineered construct over time.

**Methods:** Artificial tissue constructs called RAFTs (produced by suspension of keloid or normal dermal fibroblasts in type I collagen gel with an overlying keratinocyte layer) were cultured at air-fluid interface. Multiphoton microscopy SHG images of collagen in the intact tissue

constructs consisting of normal or keloid-derived fibroblasts were obtained. The constructs were then incised with a scalpel. Serial MPM and phase-contrast microscopy images were obtained to monitor changes in the extracellular matrix in response to wounding of the artificial skin construct over 8 days.

**Results:** The tissue-engineered constructs formed a bilayer resembling the dermis and epidermis of human skin. Phase-contrast microscopy revealed migration of keratinocytes into the defect created by scalpel wounding. The constructs were found to contract with time after wounding. The MPM SHG images showed collagen deposition in the tissue constructs after wounding. Tissue constructs with keloid-derived fibroblasts were found to deposit collagen at a higher rate than those with normal fibroblasts.

**Conclusions:** The MPM model described herein permits serial observation of the same intact specimens without the need for fixation or cytotoxic stains. Furthermore, it demonstrates the biologic activity of RAFT artificial tissue constructs.

*Arch Facial Plast Surg. 2004;6:180-187*

**W**OUND HEALING IS A physiologic process that repairs discontinuities and tissue defects produced by trauma or surgery. Fibroblasts restore mechanical stability of wounds by producing collagen, fibronectin, elastin, and peptidoglycan to replace damaged tissue with scar. Keloids and hypertrophic scars result from excessive collagen production in response to an injury and frequently result in cosmetically and functionally unacceptable scars. Keloids differ from hypertrophic scars in that keloids grow outside of the boundaries of wounds, whereas hypertrophic scars remain confined to the injury or incision margin. Prevention and/or treatment of ab-

errant wound healing continues to be a challenge to surgeons.

Fibroblasts derived from keloids and hypertrophic scars have been studied using many different laboratory models. In vitro studies of keloid-derived fibroblast metabolism have identified increased collagen, fibronectin, elastin, and peptidoglycan production.<sup>1,2</sup> More recent studies have identified phenotypic differences in growth factor production, receptor expression, and intracellular signal transduction between normal, keloid, and hypertrophic scar fibroblasts.<sup>3-7</sup> These investigations have focused on studying fibroblast behavior using cell proliferation assays and biochemical assays such as tritiated proline incorporation, procollagen

Author affiliations are listed at the end of this article.

messenger RNA production, or growth factor production assays to investigate differences in biosynthetic activity between various types of fibroblasts in standard tissue cultures. Some investigators have developed methods to study fibroblast behavior in response to injury and have shown that fibroblasts in modified Petri dish cultures respond to injury by producing collagen and/or growth factors.<sup>8</sup> Such assays typically require destruction of the extracellular matrix and/or cell lysis to allow measurements to be performed and, hence, do not allow serial examination of a single specimen or culture over time.

Recently, the RAFT organotypic culture model<sup>4,9-11</sup> has been developed to study wound healing. A RAFT is an artificial tissue model consisting of fibroblasts embedded in a collagen gel with or without keratinocytes seeded on the surface. The RAFT cultures with keratinocytes resemble skin and simulate the extracellular matrix and native environment of fibroblasts.<sup>9</sup> This provides a more natural growth environment in which to investigate fibroblast activity. **Figure 1** depicts the layers, cellular components, and extracellular matrix of a RAFT tissue construct. Despite these advantages, studies using RAFT cultures *without a keratinocyte layer* to investigate keloid biology have continued to use destructive methods that require dissolution of the RAFT cultures to monitor fibroblast activity.<sup>10,11</sup> However, under clinical conditions, keloids and hypertrophic scars evolve over time. Thus, the value and importance of a model that permits serial examination of fibroblasts derived from these lesions cannot be overstated.

Multiphoton microscopy (MPM) is an emerging imaging technique with many advantages over conventional confocal and electron microscopy. Multiphoton microscopy does not require fixation and section of tissues or use of dyes, stains, or other exogenous additives for imaging. Optical contrast in these images is produced by endogenous fluorophores, primarily nicotinamide adenine dinucleotide hydrogenase and/or nicotinamide adenine dinucleotide phosphate, riboflavin, and matrix collagen fibers. Thus, MPM can be used to produce nondestructive optical sections of living tissues with diffraction-limited image resolution. Multiphoton microscopy and its applications have been reviewed in detail by Emptage,<sup>12</sup> White and Errington,<sup>13</sup> and Halbhauer and Konig.<sup>14</sup> Recently, the use of second harmonic generation (SHG) has been shown to produce images of collagen structure in the extracellular matrix. Mohler et al,<sup>15</sup> Zoumi et al,<sup>16</sup> and Zipfel et al<sup>17</sup> have described the use of SHG in detail.

In the present study, we use MPM to produce SHG images of collagen fiber density in RAFT tissue constructs prepared with native or keloid-derived fibroblasts. The tissue constructs were wounded using surgical scalpels to create a tissue-engineered wound model. Changes along the incision site were imaged over time. Second-harmonic-generation images and signal intensity were used to determine the changes in collagen density.

## METHODS

### FIBROBLAST CULTURE

Human fibroblasts were isolated from surgical specimens under protocols approved by the University of California Irvine institutional review board. Primary tissues included neonatal fore-



**Figure 1.** Digital photomicrograph of a RAFT tissue construct showing resemblance to skin. Note the 2-layered structure of the RAFT with stratification of the keratinocyte layer and fibroblasts within the collagen layer (hematoxylin-eosin, original magnification  $\times 10$ ).

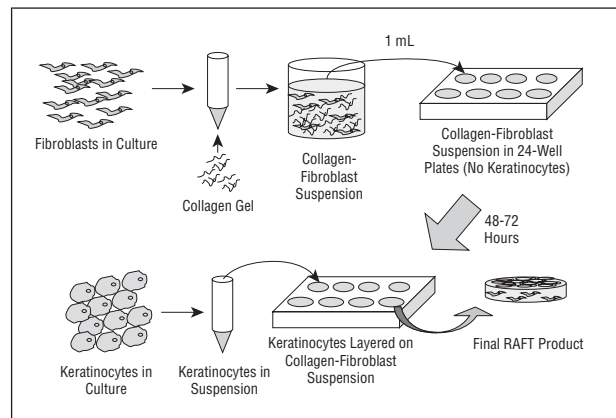


**Figure 2.** Schematic of construction of RAFT tissue constructs.

skin and keloids. Fibroblasts were serially expanded in flasks (Falcon T25, T50 and T75; Becton-Dickinson, Franklin Lakes, NJ) containing Dulbecco modified Eagle medium supplemented with 1% L-glutamine, 1% penicillin-streptomycin, and 10% fetal bovine serum (fibroblast growth medium). Cells in confluent culture were released with 0.25% trypsin/0.5% EDTA solution, then resuspended in fibroblast growth medium and placed in larger flasks. All cultures were maintained in identical conditions in incubators at 37°C and 7.5% carbon dioxide.

### KERATINOCYTES

Keratinocytes isolated from neonatal foreskin were serially expanded in keratinocyte growth medium supplemented with 0.06mM calcium ion ( $\text{Ca}^{2+}$ ) solution (**Figure 2**) (KGM-2; Clonetics, East Rutherford, NJ). At confluence, cells were re-

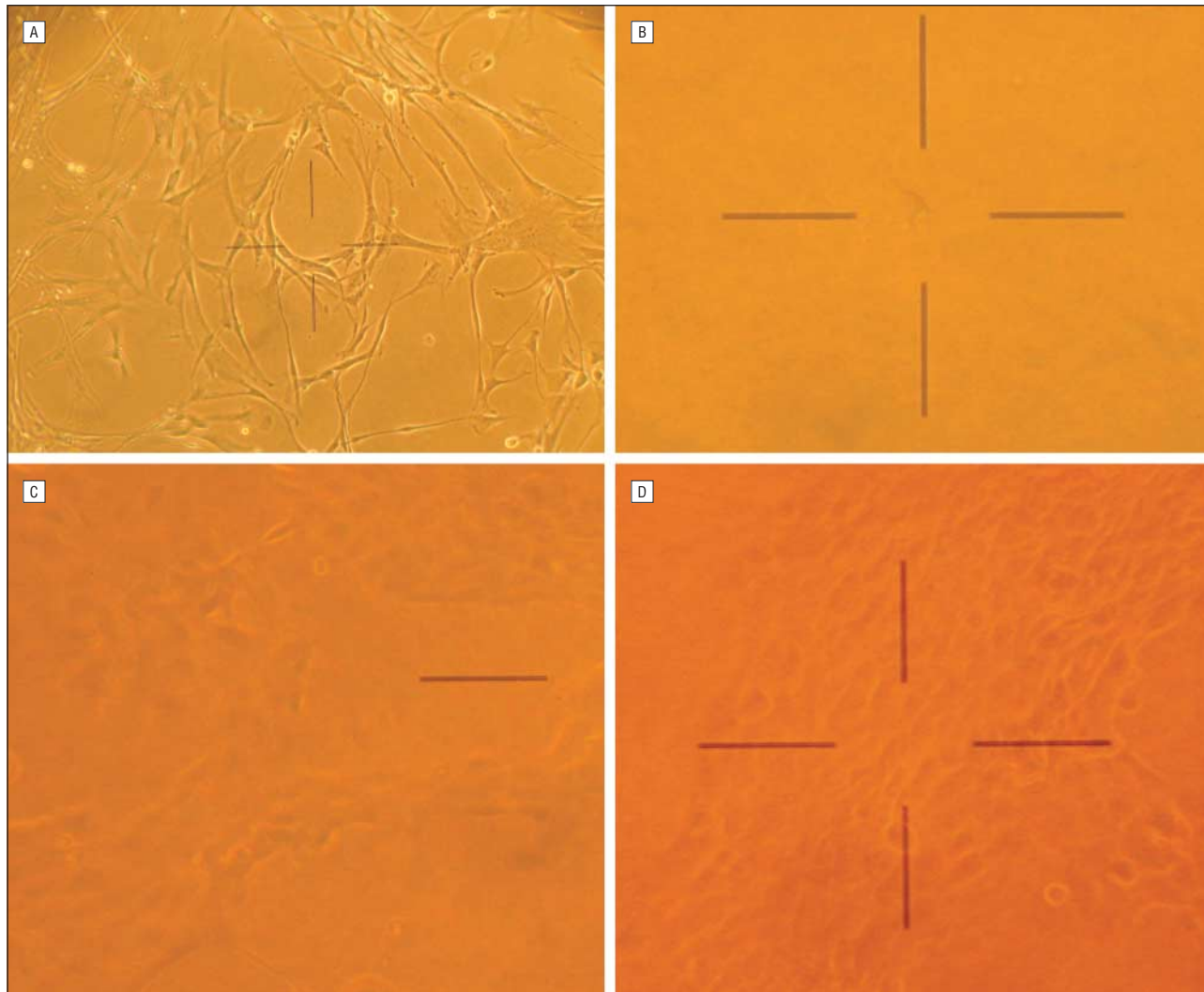


**Figure 3.** Digital photomicrographs: A, fibroblasts in cell culture; B, fibroblast within a RAFT tissue construct; C, keratinocytes on the surface of a RAFT tissue construct 1 day after seeding onto the surface; and D, keratinocytes on a RAFT surface 4 days after seeding onto the surface.

leased with 0.25% trypsin/0.5% EDTA, which was then neutralized with trypsin neutralizing solution (TNS; Fisher Scientific, Pittsburgh, Pa). Once at confluence in T75 flasks, cells were released from culture flasks and used to seed the epithelial layer of the RAFT tissue constructs.

#### RAFT TISSUE CONSTRUCTS

A schematic representation of RAFT construction is provided in Figure 2. After expansion and release, fibroblasts were suspended in 10 mL of fibroblast growth medium in a centrifuge tube, and cell density was estimated using an electronic cell counter (Model Z1; Beckman Coulter, Fullerton, Calif). Then  $10^6$  cells were removed, placed in a separate tube, and centrifuged at 1000 rpm for 8 minutes to obtain a pellet. The pellet was then resuspended in  $\times 5$  high-glucose-concentration Dulbecco modified Eagle medium and added to a collagen gel mixture consisting of 65% rattail collagen type I (3.67 mg/mL) in 0.02N glacial acetic acid (BD Biosciences, Bedford, Mass), 20%  $\times 5$  high-glucose Dulbecco modified Eagle medium, 10% (vol/vol) reconstitution buffer (260mM sodium carbonate and 200mM HEPES [*N*-2-hydroxyethylpiperazine-*N'*-2-ethanesulfonic acid] buffer in 0.05N sodium hydroxide) to obtain a final concentration of  $10^5$  cells/mL of the gel. This collagen-fibroblast suspension was transferred into wells in a 24-well

tissue culture plate (1 mL of suspension per well) and incubated for 20 minutes at 37°C and 7.5% carbon dioxide. Then an additional 1 mL of fibroblast growth medium was added to each well, and the plates were returned to the incubator.

Over the following 48 to 72 hours, the culture medium within the wells was changed to KGM-2 by gradual dilution of the fibroblast growth medium. A phase-contrast microscope was used to monitor the fibroblasts after suspension and to ensure that they had assumed a spindle-shaped structure within the collagen gel as is generally observed in fibroblasts in culture (**Figure 3A** and **B**). Seventy-two hours after the construction of the collagen-fibroblast suspension, keratinocytes in culture flasks were released, diluted to the appropriate dilution, and seeded ( $10^5$  cells/well) to the top layer of the collagen-fibroblast gel. The wells containing the completed bilayer RAFT constructs were then filled with KGM-2 supplemented with 0.06mM  $Ca^{2+}$ . Wells were returned to the incubator and evaluated periodically over the next 72 hours using phase-contrast microscopy to monitor keratinocyte adhesion to the collagen-fibroblast gel and growth (**Figure 3C** and **D**). All 24-well plates were incubated in identical conditions at 37°C and 7.5% carbon dioxide.

Once the cells had reached confluence on the surface of the constructs, the growth medium was changed to KGM-2 supplemented with 0.9mM  $Ca^{2+}$ <sup>18</sup> to promote keratinocyte differentiation and stratification. At this time, the tissue con-

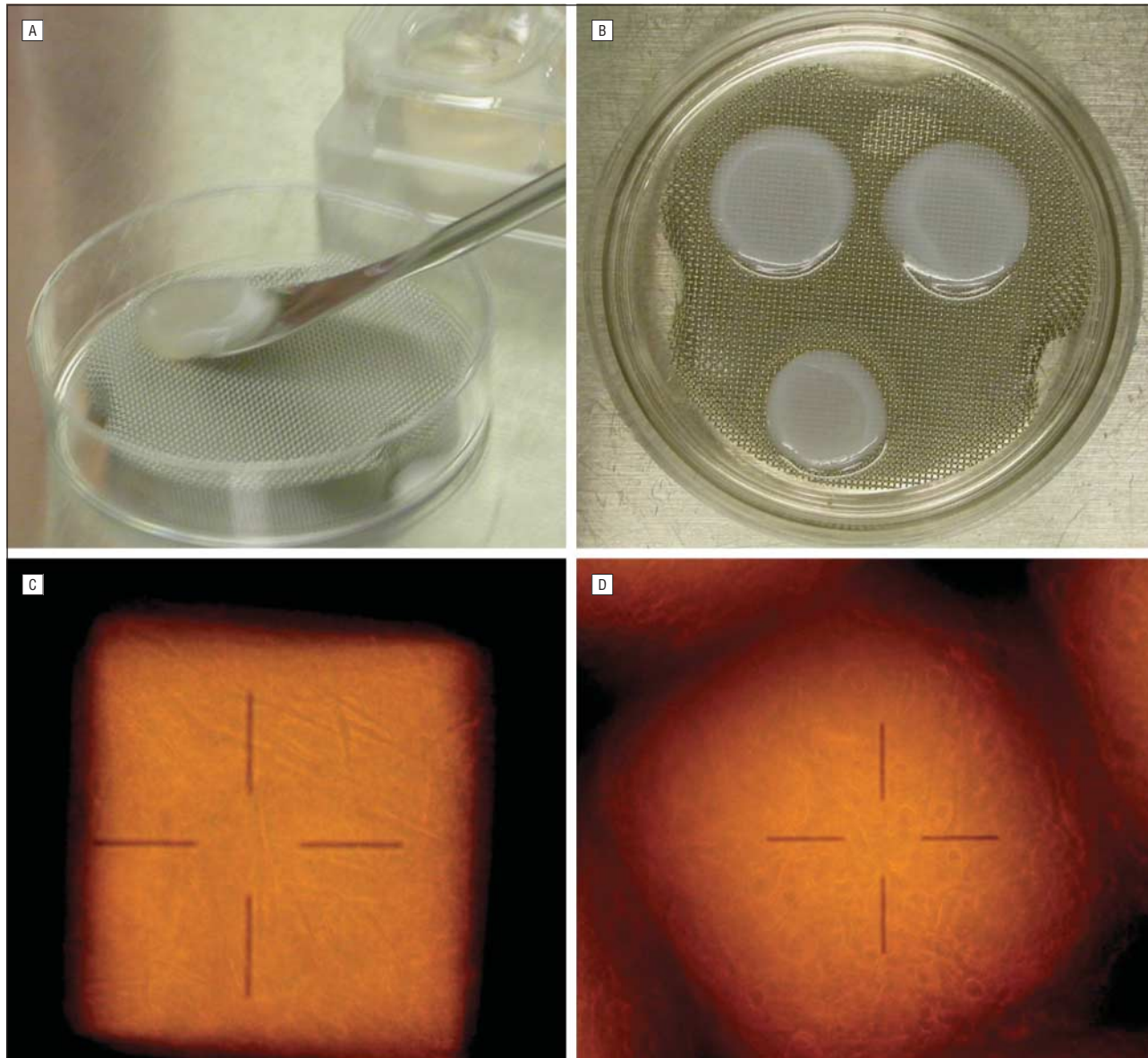


**Figure 4.** A, Placement of RAFT onto elevated stainless steel mesh; B, RAFT cultures at air-fluid interface; C, digital phase-contrast photomicrograph of RAFT focused on fibroblast layer through stainless steel mesh; and D, digital phase-contrast photomicrograph of RAFT focused on keratinocyte layer through stainless steel mesh and depicting stratification of keratinocytes.

structs were transferred from the 24-well plates to Petri dishes fitted with elevated sterile stainless steel mesh (**Figure 4A**). The tissue constructs were placed on the elevated mesh. The Petri dishes were then filled with KGM-2 supplemented with 0.9mM  $Ca^{2+}$  up to the level of the elevated mesh to allow incubation of the tissue constructs with an air-fluid interface (**Figure 4B**). The tissue constructs were then evaluated with phase-contrast microscopy over several days. Multiphoton microscopy imaging started once the keratinocyte layer was observed to stratify into multiple layers (**Figure 4C and D**). Some of the RAFTs were found to be contaminated with hyphated fungal organisms and were discarded.

#### WOUNDING OF CONSTRUCTS

Once stratification of the keratinocyte layer had occurred, the artificial skin constructs were incised with No. 10 surgical blades (Bard & Parker, Franklin Lakes, NJ). Incisions were made in the center of the tissue constructs by hand and carried through

the full thickness of each construct (**Figure 5**). The tissue-engineered constructs were maintained at air-fluid interface under identical culture conditions. Wounded and native tissue constructs of keloid and normal fibroblasts were maintained in separate culture dishes to avoid soluble growth factors or autocrine regulators from intermixing.<sup>3,19,20</sup>

#### PHASE-CONTRAST MICROSCOPY

Phase-contrast microscopy was performed with Carl Zeiss AxioStar Plus and Axiovert S1002TV model microscopes (Plus, Munich, Germany). Digital images were recorded directly through the microscope eyepiece using a digital camera (Coolpix 4500; Nikon, Tokyo, Japan) without the use of an adapter. Digital images were analyzed and enhanced using Adobe Photoshop software (Adobe, San Jose, Calif). Microscopy of RAFT tissue constructs using these microscopes allowed us to observe different layers of the constructs by modification of the depth of focus (**Figure 4C and D**).

## MULTIPHOTON MICROSCOPY

The multiphoton microscope used in this study consists of a mode-locked, 150-femtosecond titanium:sapphire laser used at a 76-MHz repetition rate (Mira 900F; Coherent, Santa Clara, Calif) pumped by a 5-W Verdi laser (Coherent). The titanium:sapphire laser beam is deflected into the back port of an inverted Zeiss Axiovert S1002TV microscope (Zeiss, Thornwood, NY) using a personal computer-controlled, galvanometer-driven X-Y scanner (Series 603X; Cambridge Technology, Inc, Watertown, Mass). This beam is deflected by a short-pass dichroic mirror, which maximizes reflection in the infrared and transmission in the blue-green region of the spectrum and is focused onto the sample through a  $\times 63$ , c-apochromat, water-immersion microscope objective. The excited fluorescence and

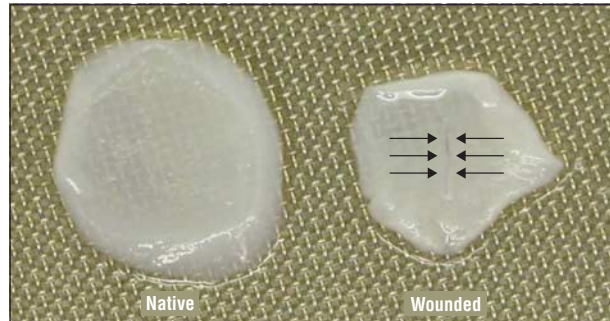


**Figure 5.** Digital image showing native and wounded RAFT tissue constructs. Arrows point to scalpel wound at the center of the RAFT.

SHG signals from the sample are discriminated using 520- and 400-nm bandpass filters (CVI Laser, Livermore, Calif), respectively, and detected by a photomultiplier tube. Images are produced as previously described.<sup>16</sup>

## MEASUREMENT OF COLLAGEN SYNTHESIS

The SHG emissions of the tissue constructs were collected as 2-dimensional images from 3 different points on the non-keratinocyte-bearing surface of each tissue construct. By changing the depth of the focal plane, images were collected up to depth of 240  $\mu\text{m}$  at intervals of 30  $\mu\text{m}$ . Digital images were recorded in data format ( $256 \times 256$  pixels, corresponding to 35  $\mu\text{m}^2$ ) and converted into TIFF images using MATLAB (The Mathworks, Natick, Mass). The images were viewed and analyzed using Photoshop software (Adobe). **Figure 6** shows digital images of SHG collected from a single RAFT showing depth-dependent decay (DDD) of the SHG signal. A numerical value for SHG intensity of each image was obtained by calculating the mean value of the intensity histogram for the entire image.

The tissue constructs were imaged on day 0, which corresponds to the day when the specimen was incised, and then imaged at 2- to 3-day intervals for 10 days. The average SHG intensity of images at each depth was then calculated. The SHG intensity was plotted as a function of depth, and a curve for each day was generated for each RAFT specimen. A sample is shown in **Figure 7**. Decrease in SHG signal intensity with increasing depth can be approximated using a first-order model:  $y = Ae^{-\kappa x} + C$ , where  $y$  is the SHG intensity,  $x$  is the depth from the specimen surface,  $\kappa$  is the DDD constant,  $A$  is a pre-exponential scaling factor, and  $C$  is an arbitrary constant that

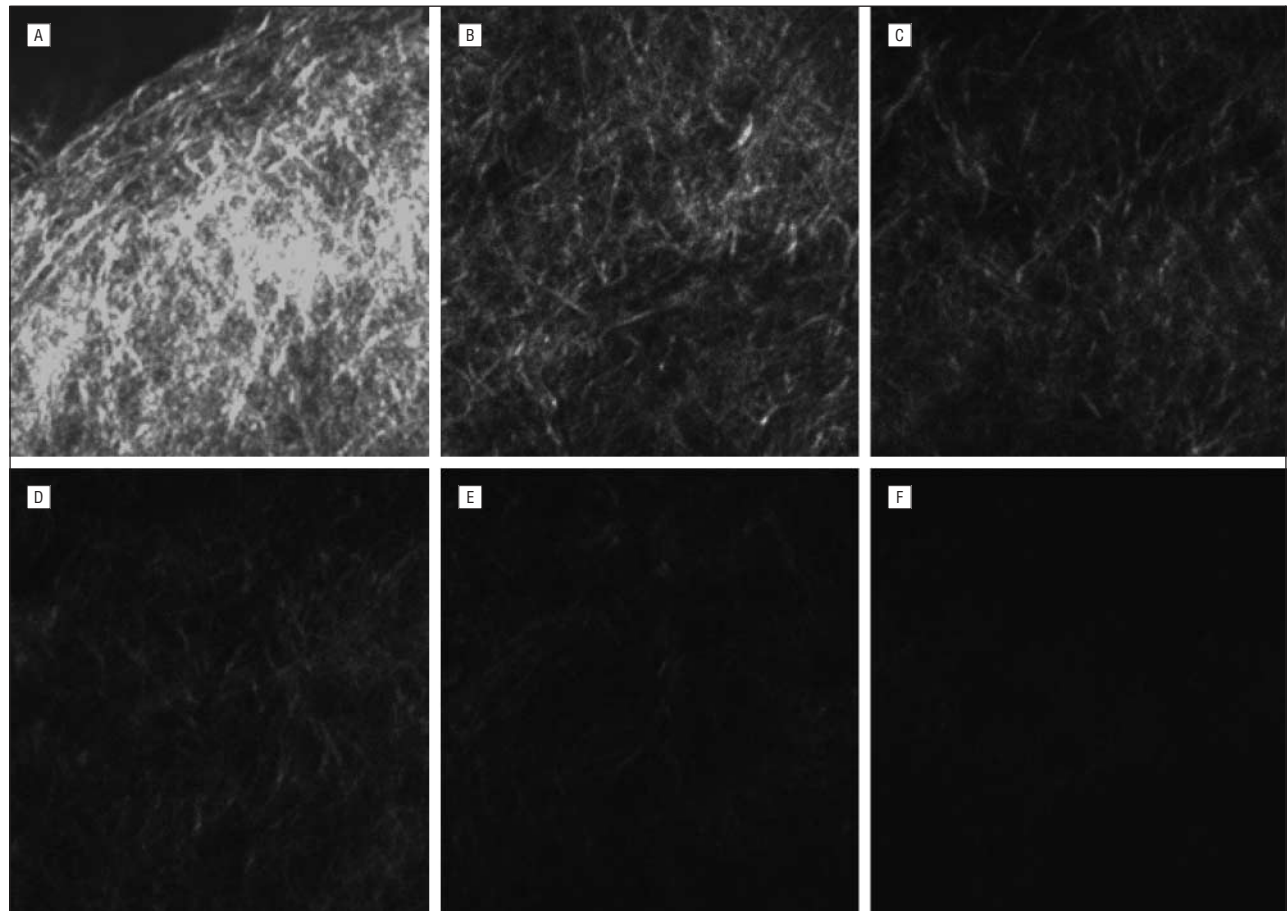


**Figure 6.** Multiphoton second-harmonic-generation images of a RAFT tissue construct at different depths of focus: A, 0  $\mu\text{m}$ ; B, 30  $\mu\text{m}$ ; C, 60  $\mu\text{m}$ ; D, 90  $\mu\text{m}$ ; E, 120  $\mu\text{m}$ ; and F, 150  $\mu\text{m}$ .

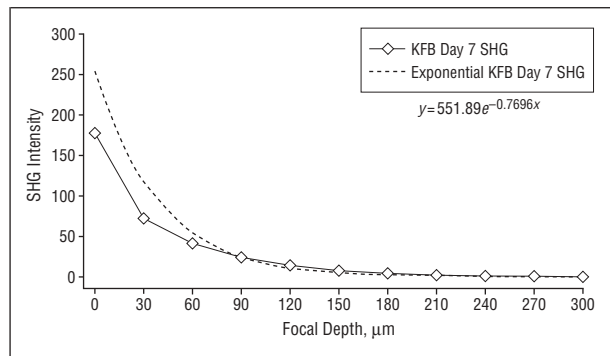


**Figure 7.** Sample graph of second-harmonic-generation (SHG) signal intensity against depth of focus. The dotted line depicts the best-fit exponential decay curve. The equation used to determine the decay constant ( $\kappa$  value) is shown. KFB indicates keloid fibroblast RAFT construct.

adjusts the SHG signal intensity at the greatest depth to zero. The decay constant was calculated using Microsoft Excel spreadsheet software (Microsoft, Redmond, Wash).

## RESULTS

### OBSERVATIONS OF THE TISSUE CONSTRUCTS

Fibroblasts within the tissue constructs observed with phase-contrast microscopy immediately after suspension in the collagen gel were noted to be rounded (**Figure 8A**). Serial observation demonstrated a change in cell structure from rounded to spindle shaped, which indicates integration into the collagen matrix (Figure 8B). Both native and keloid-derived fibroblast constructs were observed to contract over time (**Figure 9**).

The scalpel incisions in the constructs were observed over time grossly and using phase-contrast microscopy. Depth of focus was changed to identify either the superficial keratinocytes or fibroblasts located deep within the constructs. Cells at the edge of the scalpel wounds assumed rounded shape as determined by both phase-contrast microscopy and MPM (**Figure 10**). Both keratinocytes and fibroblasts at the surface of the constructs were noted to migrate to the center of the wound in both types of tissue constructs. Scalpel wounds were translucent on gross inspection in the period immediately after wounding. Eight to 10 days after wounding, these translucent areas were less detectable to the unaided eye (**Figure 11**).

### COLLAGEN DENSITY AND DDD

Second-harmonic-generation intensity decreased exponentially with increasing depth in all RAFT tissue constructs. A sample graph of DDD and calculation of the decay constant is shown in Figure 7. The DDD increased with collagen density and was observed to increase over time in both keloid and normal tissue constructs. Decay-constant ( $\kappa$ ) values determined for each type of fibroblast construct were larger in keloid-derived constructs than in normal constructs ( $P = .05$ , 2-tailed  $t$  test) at each time interval measured after wounding (**Figure 12**).

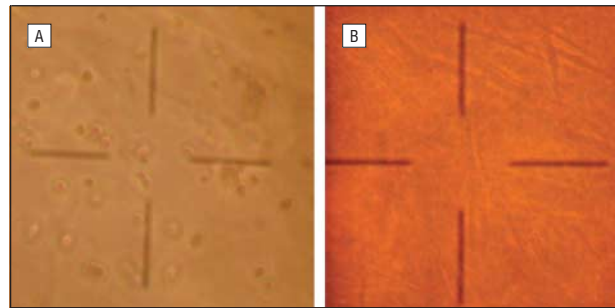


**Figure 8.** Phase-contrast digital photomicrographs of fibroblasts in collagen gel immediately after suspension (A) and 4 days after suspension (B).

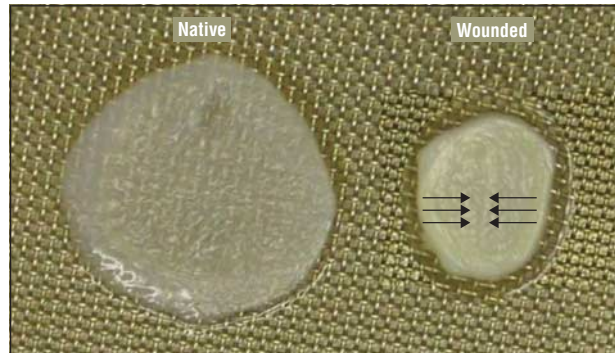


**Figure 9.** Native and wounded RAFT tissue constructs approximately 12 days after wounding. The arrows indicate the scalpel wound, which appears as a thickened area within the contracted RAFT.

## COMMENT

In this study, we describe a novel model for the investigation of aberrant wound healing using organotypic tissue-engineered cultures and MPM. The data presented are in accord with previous work using conventional methods that have shown that keloid-derived fibroblasts exhibit phenotypic differences resulting in increased collagen production.<sup>1-7</sup>

The advantage of the present system is that it incorporates a biologically active wound model resembling human skin with an imaging device that allows serial measurements of the same specimen over time. Furthermore, since MPM provides a quantitative measurement of collagen second harmonic signal generation, it can be used to estimate matrix collagen density without fixation or exogenous dyes that could cause disruption of the native physiologic environment. The use of RAFT tissue constructs allows observation of both cell (fibroblasts and keratinocytes) and matrix behavior in response to injury or changes in cytokines or the physical milieu. The potential impact of this system in studying hypertrophic scars, keloids, and other aberrant wound-healing mechanisms is clear. Additionally, since serum-free<sup>3,19,20</sup> media are used, MPM studies can be combined with classic techniques when more biochemical detail is required.

Conventional phase-contrast microscopy of the RAFT tissue constructs allows one to visualize the biologic activity of the wound, as shown in Figures 2 through 7. Keratinocytes and fibroblasts along the wound edge were observed to change shape and structure; a clear sign of the

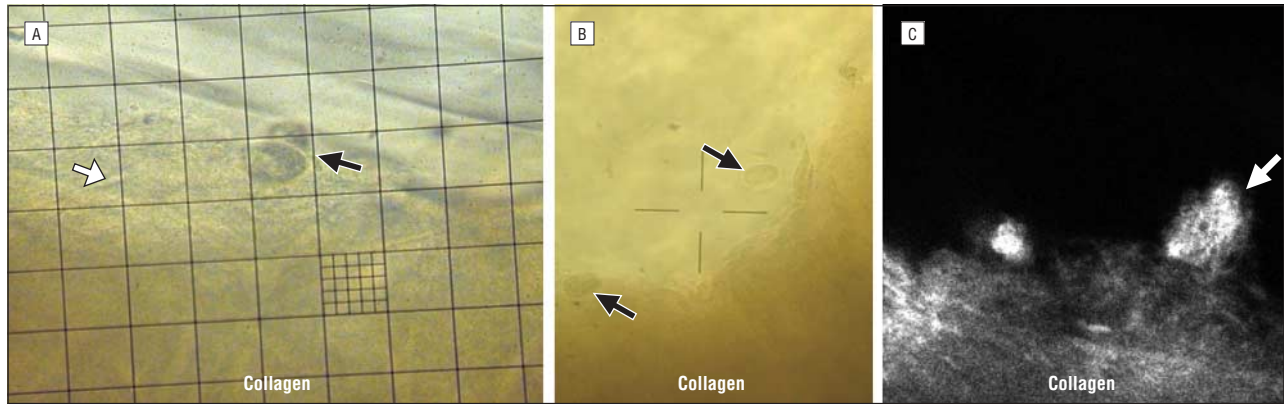


**Figure 10.** A and B, Digital phase-contrast photomicrographs of the wound edge: the black arrows show rounded fibroblasts migrating into wound edge; the white arrow (A) shows a spindle-shaped fibroblast in collagen suspension. C, Multiphoton fluorescent microscopic image of fibroblasts migrating into the wound edge and collagen at the wound edge; arrow shows a rounded fibroblast migrating into the wound edge.

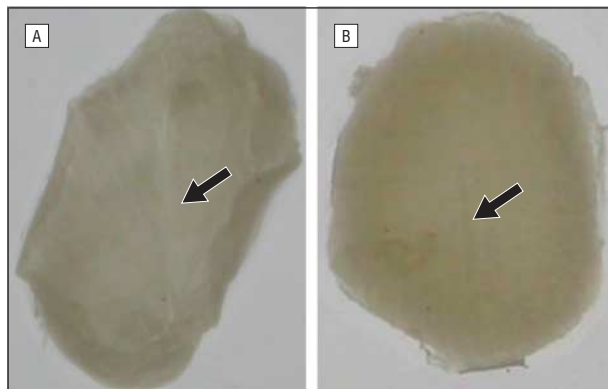


**Figure 11.** Digital photographs of wounded RAFT tissue constructs 3 days (A) and 12 days (B) after wounding. Arrows point to the scalpel wounds at the center of the constructs.

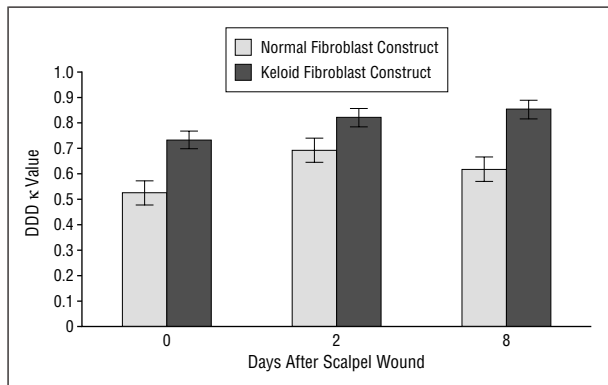


**Figure 12.** Depth-dependent decay constant (DDD  $\kappa$  value) against time.

biologic response to wounding. This observation is also seen in direct MPM images of cells and in the increased collagen density as measured by DDD in response to wounding. The MPM images from areas within the RAFTs adjacent to the wound edge show cells surrounded by collagen fibers, which suggests increased synthesis in response to injury. Multiphoton microscopy allows visualization of biologic changes in these living specimens.

One limitation in the present RAFT model is related to the physical transfer of specimens from the culture dish to the vestibule for imaging in the MPM de-

vice. The RAFTs are removed from the incubator for approximately 30 to 45 minutes each time imaging is performed and transferred to sterile, covered, glass-bottomed dishes using a sterilized spatula in a laminar flow hood (Figure 5). However, the environment of the MPM device where imaging and data collection are performed exposes the tissue to ambient environmental conditions. As a consequence, some of the tissue constructs became contaminated with fungus at approximately 14 days after first exposure.

The transfer of specimens back and forth between the culture and imaging dishes also identified a technical challenge related to wound depth. Full-thickness incisions of the constructs were made, which resulted in partial separation when the specimen was moved. The net effect of these maneuvers was to produce repeated injury. Likewise, imaging within the wound gap would affect the measurement of DDD of SHG. Hence, care was taken to collect images from within intact regions of the tissue constructs. Future studies now under way will use a servo-controlled instrument to create wounds with consistent depth that do not span the full thickness of the specimen.

The measurement of the DDD of SHG signal assumes that (1) the DDD is the same in unwounded RAFTs constructed with either keloid or normal fibroblasts and (2) the transmission of near-infrared light in RAFT tissue constructs is absorption dominated. The latter concept has been explored in detail by Dunn et al,<sup>21</sup> who found that although scattering plays a role in DDD, absorption is the main factor responsible for DDD in turbid media at least to a depth of focus of 412  $\mu\text{m}$ . Thus, although DDD is not a perfect measure, it is a reasonable measure of collagen fiber density, certainly to the depths examined in the present study.<sup>21</sup> We observed a statistically significant difference in DDD and  $\kappa$  between RAFT tissue models constructed with keloid-derived or normal fibroblasts. This correlates with clinical observations of keloid behavior and findings of other in vitro studies investigating collagen deposition by normal or keloid fibroblasts after wounding.<sup>1,8</sup>

In conclusion, we have described a wound-healing model and imaging system that allows the measurement of collagen production in organotypic tissue-engineered constructs resembling human skin in living specimens. Fi-



broblasts were observed to aggregate along incision line margins, and MPM SHG images identified enhanced collagen production at this interface. Imaging the collagen SHG signal in living tissues allows a direct and quantitative measure of the density of this key extracellular matrix component that is an integral part of wound healing. In contrast, DDD measurements provide a global measurement of collagen density in any user-defined optical section within the tissue and can be used to estimate the integrated response of a living tissue specimen to injury. This model is useful for serial long-term studies of wound healing. This model may prove useful in the study of potential treatments for wounds characterized by excessive and undesirable collagen deposition. Our goals in development of this model include its use in the investigation of pharmacologic and cytokine-based treatments of aberrant wound healing. The specimens in this model may be observed serially for a substantial period of time without the need for destructive measurement techniques, which allows more meaningful evaluation of potential treatments not yet used in humans.

Accepted for publication September 5, 2003.

From Departments of Otolaryngology–Head and Neck Surgery (Drs Torkian and Wong) and Biomedical Engineering (Drs Tromberg and Wong), University of California, Irvine Medical Center, Orange; Beckman Laser Institute, University of California, Irvine (Drs Yeh, Sun, Tromberg, and Wong and Mr Engel). Dr Yeh is currently at the Department of Biomedical Engineering, Texas A&M University, College Station. Mr Engel is currently a medical student at Albert Einstein School of Medicine, Yeshiva University, Bronx, NY.

This research was supported by grants RR01192 and DC 00170 from the National Institutes of Health and grant F49620-00-1-0371 from the Air Force Office of Scientific Research. The opinions or assertions contained herein are the private views of the authors and are not to be construed as official, or as reflecting the views of the US Air Force or the Department of Defense.

This work was presented at the American Academy of Facial Plastic and Reconstructive Surgery annual meeting; September 18, 2003; Orlando, Fla.

The keloid specimens were provided by Diana Mes-sadi, DDS.

The photograph for Figure 1 was taken by Bunsho Kao, MD.

We thank Hongrui Li, MD, and Tatiana Krasieva, PhD, for their technical assistance.

Corresponding author and reprints: Brian J. F. Wong, MD, PhD, Beckman Laser Institute, University of California Irvine, 1002 Health Sciences Rd E, Irvine, CA 92612 (e-mail: bjwong@uci.edu).

## REFERENCES

1. Uitto J, Perejda AJ, Abergel RP, Chu ML, Ramirez F. Altered steady-state ratio of type I/III procollagen mRNAs correlates with selectively increased type I collagen biosynthesis in cultured keloid fibroblasts. *Proc Natl Acad Sci U S A*. 1985; 82:5935-5939.
2. Babu M, Diegelmann R, Oliver N. Fibronectin is overproduced by keloid fibroblasts during abnormal wound healing. *Mol Cell Biol*. 1989;9:1642-1650.
3. Hanasono MM, Kita M, Mikulec AA, Lonergan D, Koch RJ. Autocrine growth factor production by fetal, keloid, and normal dermal fibroblasts. *Arch Facial Plast Surg*. 2003;5:26-30.
4. Tuan TL, Wu H, Huang EY, et al. Increased plasminogen activator inhibitor-1 in keloid fibroblasts may account for their elevated collagen accumulation in fibrin gel cultures. *Am J Pathol*. 2003;162:1579-1589.
5. Szulgit G, Rudolph R, Wandel A, Tenenhaus M, Panos R, Gardner H. Alterations in fibroblast alpha1beta1 integrin collagen receptor expression in keloids and hypertrophic scars. *J Invest Dermatol*. 2002;118:409-415.
6. Younai S, Nichter LS, Wellisz T, et al. Modulation of collagen synthesis by transforming growth factor-beta in keloid and hypertrophic scar fibroblasts. *Ann Plast Surg*. 1994;33:148-151.
7. Peltonen J, Hsiao LL, Jaakkola S, et al. Activation of collagen gene expression in keloids: co-localization of type I and VI collagen and transforming growth factor beta-1 mRNA. *J Invest Dermatol*. 1991;97:240-248.
8. Calderon M, Lawrence WT, Banes AJ. Increased proliferation of fibroblasts wounded in vitro. *J Surg Res*. 1996;61:343-347.
9. Kao B, Kelley KM, Majaron B, Nelson JS. Novel model for evaluation of epidermal preservation and dermal collagen remodeling following photorejuvenation of human skin. *Lasers Surg Med*. 2003;32:115-119.
10. Chipev CC, Simon M. Phenotypic differences between dermal fibroblasts from different body sites determine their responses to tension and TGF alpha-1. *BMC Dermatol*. 2002;2:13.
11. Phan TT, Li S, Bay BH, Chan SY, Lee ST. Dietary compounds inhibit proliferation and contraction of keloid and hypertrophic scar-derived fibroblasts in vitro: therapeutic implication for excessive scarring. *J Trauma*. 2003;54:1212-1224.
12. Emptage NJ. Fluorescent imaging in living systems. *Curr Opin Pharmacol*. 2001; 1:521-525.
13. White N, Errington R. Multi-photon microscopy: seeing more by imaging less. *Biotechniques*. 2002;33:298-300, 302, 304-305.
14. Halhuber KJ, Konig K. Modern laser scanning microscopy in biology, biotechnology and medicine. *Ann Anat*. 2003;185:1-20.
15. Mohler W, Millard AC, Campagnola PJ. Second harmonic generation imaging of endogenous structural proteins. *Methods*. 2003;29:97-109.
16. Zoumi A, Yeh A, Tromberg BJ. Imaging cells and extracellular matrix in vivo by using second-harmonic generation and two-photon excited fluorescence. *Proc Natl Acad Sci U S A*. 2002;99:11014-11019.
17. Zipfel WR, Williams RM, Christie R, Nikitin AY, Hyman BT, Webb WW. Live tissue intrinsic emission microscopy using multiphoton-excited native fluorescence and second harmonic generation. *Proc Natl Acad Sci U S A*. 2003;100: 7075-7080.
18. Vespa A, Darmon AJ, Turner CE, D'Souza SJ, Dagnino L. Ca<sup>2+</sup>-dependent localization of integrin-linked kinase to cell junctions in differentiating keratinocytes. *J Biol Chem*. 2003;278:11528-11535.
19. Hong RH, Lum J, Koch R. Growth of keloid-producing fibroblasts in commercially available serum-free media. *Otolaryngol Head Neck Surg*. 1999;121:469-473.
20. Koch RJ, Goode RL, Simpson GT. Serum-free keloid fibroblast cell culture: an in vitro model for the study of aberrant wound healing. *Plast Reconstr Surg*. 1997; 99:1094-1098.
21. Dunn AK, Wallace VP, Coleno M, Berns MW, Tromberg BJ. Influence of optical properties on two-photon fluorescence imaging in turbid samples. *Appl Opt*. 2000; 39:1194-1201.